

IT'S ALIVE! THE SUPERNOVA IMPOSTOR 1961V

SCHUYLER D. VAN DYK

Spitzer Science Center, Caltech, 220-6, Pasadena, CA 91125

AND

THOMAS MATHESON

National Optical Astronomy Observatory, 950 North Cherry Avenue, Tucson, AZ 85719

To Appear in ApJ.

ABSTRACT

Reports of the death of the precursor of Supernova (SN) 1961V in NGC 1058 are exaggerated. Consideration of the best astrometric data shows that the star, known as “Object 7,” lies at the greatest proximity to SN 1961V and is the likely survivor of the “SN impostor” super-outburst. SN 1961V does not coincide with a neighboring radio source and is therefore not a radio SN. Additionally, the current properties of Object 7, based on data obtained with the *Hubble Space Telescope*, are consistent with it being a quiescent Luminous Blue Variable (LBV). Furthermore, post-explosion non-detections by the *Spitzer Space Telescope* do not necessarily and sufficiently rule out a surviving LBV. We therefore consider, based on the available evidence, that it is yet a bit premature to reclassify SN 1961V as a *bona fide* SN. The inevitable demise of this star, though, may not be too far off.

Subject headings: supernovae: general — supernovae: individual (SN 1961V) — stars: evolution — stars: variables: other — galaxies: individual (NGC 1058) — galaxies: stellar content

1. INTRODUCTION

The evolution of the most massive stars is not well known. It is thought that main sequence stars with $M_{\text{ZAMS}} \gtrsim 30 M_{\odot}$ proceed through a blue supergiant phase, possibly to a red supergiant phase, or straight to a luminous blue variable (LBV) phase, and to the Wolf-Rayet (WR) phase prior to explosion as supernovae (SNe). That WR stars typically possess $M \lesssim 20 M_{\odot}$ (Crowther 2007) requires their precursor stars to shed most of their mass, presumably through eruptive mass ejections as a LBV (Humphreys & Davidson 1994; Smith & Owocki 2006). The term “supernova impostor” has been coined (Van Dyk et al. 2000) to describe these eruptive events for massive stars, such as η Carinae (e.g., Davidson & Humphreys 1997). This is because various observational aspects of the eruptions can mimic the properties of true SNe. During η Car’s Great Eruption in the 1800s, the star greatly exceeded the Eddington limit, with the bolometric luminosity increasing by ~ 2 mag. The total luminous output of such an eruption ($\sim 10^{49}$ – 10^{50} erg) can rival that of a SN.

However, a SN, by strict definition, is an explosive event that ends the life of a star (although a compact object may form in the process). If an optical transient is observed with energetics comparable to that of a true SN, and, after a sufficient period of time has elapsed, a star still exists at the exact position of the transient, then that transient is a SN impostor.

The most studied example of a SN impostor, SN 1961V in NGC 1058, remains controversial to this day. A debate has continued as to whether or not this event was a true SN. In fact, it is truly impressive how many journal pages have been spent on this one object. This includes two recent studies, both of which present arguments that claim SN 1961V as a genuine SN. We argue here that SN 1961V is an impostor and that its precursor has survived

what was a powerful eruption. Many of our points below were first presented in our review of SN impostors (Van Dyk & Matheson 2011).

2. SUPERNOVA OR SUPERNOVA IMPOSTOR?

We only briefly summarize the history of observations of SN 1961V and the debate. We encourage the reader to peruse the original papers for more detailed discussions, which include (but are not limited to) Goodrich et al. (1989), Humphreys & Davidson (1994), Filippenko et al. (1995), Humphreys, Davidson, & Smith (1999), Chu et al. (2004), Van Dyk (2005), Smith et al. (2011), and Kochanek, Szczygiel, & Stanek (2011). While reading this summary, please keep in mind that the most accurate astrometry inevitably shows that the source “Object 7” (Filippenko et al. 1995) is most coincident with SN 1961V, and that the centroid of detected radio emission is offset from this position. See Figure 1.

The photographic light curve for SN 1961V has been characterized as “strange” (Bertola 1964; Branch & Greenstein 1971). The progression of the outburst is described by Humphreys & Davidson (1994, their Table 3) and shown schematically by, e.g., Goodrich et al. (1989). Additionally, the long-term photometric monitoring (Bertola 1965) of SN 1961V showed that its color remained relatively constant, abnormally resembling that of an F supergiant ($B - V \approx 0.6$ mag). The SN faded below optical detectability in late 1968.

The unusual early-time optical spectra were dominated by narrow emission lines of H, He I, and Fe II, with a maximum expansion velocity of only ~ 2000 km s^{−1} (Zwicky 1964; Branch & Greenstein 1971). These spectral attributes could be considered similar to the characteristics of Type IIn SNe (SNe IIn, where “n” designates “narrow” Schlegel 1990; Filippenko 1997). For both impostors and SNe IIn the coincidence of a hydrogen envelope with simi-

lar kinetic energies results in spectra with similar appearance, specifically, strong Balmer lines, typically a narrow emission profile (with velocities $\sim 100\text{--}200\text{ km s}^{-1}$) atop an “intermediate width” base (with velocities of $\sim 1500\text{--}2000\text{ km s}^{-1}$ in the case of the SNe IIn; Smith et al. 2008). The narrow component is interpreted as emission from pre-shock circumstellar gas. The intermediate-width component for SNe IIn arises from interaction of the SN shock with the dense circumstellar matter (e.g., Turatto et al. 1993; Smith et al. 2008), which is expected to result in luminous and long-lived radio, X-ray, and optical emission (e.g., Chevalier & Fransson 1994; Chevalier 2003; although, see Van Dyk et al. 1996 regarding the radio emission). See a recent discussion of SNe IIn and their properties by Kiewe et al. (2012). For SN impostors, the intermediate-width component of the Balmer emission lines are significantly narrower than for the SNe IIn, and early-time spectra for SNe IIn generally are quite blue, whereas impostors, soon after discovery, can appear either “hot” or “cool” (Smith et al. 2011).

Both Bertola (1964) and Zwicky (1964) identified a $m_{\text{pg}} \approx 18$ mag object at the SN site in pre-SN photographic plates of the host galaxy. Zwicky noted that the star exhibited small variations for 23 years prior to rising by six magnitudes in a year, “acting similarly to η Carinae....” At the host galaxy’s distance (adopting 9.3 Mpc, the Cepheid distance to NGC 925, in the same “NGC 1023” group as NGC 1058; Silbermann et al. 1996), the presumed precursor star would have been an incredible $M_{\text{pg}} \approx -12$ mag, implying it was the most luminous known star in the local Universe. From this Utrobin (1984) modelled the SN’s peculiar light curve as the explosion of an (almost certainly improbable) 2000 M_{\odot} star.

The hunt for the remnant of this extraordinary explosion began in earnest in 1983, when Fesen (1985) identified a faint knot of $\text{H}\alpha$ emission very near the SN position, in the easternmost of two HII regions (each separated by $\sim 4''$, with $\log L_{\text{H}\alpha} \approx 37.2$; Goodrich et al. 1989). Branch & Cowan (1985) detected a source of nonthermal radio emission in 1984 with the Very Large Array (VLA), also very near the optical SN position. Klemola (1986) measured a very accurate position (uncertainty $\lesssim 0''.1$) for SN 1961V from Lick plates taken in 1961, as well as of the precursor from a plate from 1937. The conclusion that Branch & Cowan reached was that the radio emission was from an aging SN, or very young remnant, corresponding to SN 1961V. However, in very late-time optical spectra from 1986 of the SN environment, Goodrich et al. (1989) found a narrow (unresolved) $\text{H}\alpha$ emission-line profile atop an intermediate-width ($\approx 2100\text{ km s}^{-1}$ FWHM) base, at the SN position. From a comparison with the properties of known LBVs, Goodrich et al. concluded that SN 1961V was *not* a true SN, but instead was a possible “ η Car analog.” Comparing the $\text{H}\alpha$ emission they detected from SN 1961V to that from η Car, they argued that the survivor of a 1961 super-outburst lies behind high circumstellar extinction of $A_V \approx 5$ mag.

Filippenko et al. (1995) subsequently obtained *VRI* images of the SN field in 1991 with the pre-refurbishment *Hubble Space Telescope* (*HST*) Wide-Field/Planetary Camera-1 (WF/PC-1), detecting an apparent cluster of

10 stellar-like objects, all within $\sim 5''$. From those relatively low-quality data, they isolated “Object 6” in the cluster (see Figure 1) as the likely survivor of the 1961 super-outburst, although other stars in the environment could not be completely excluded based on the positions of these stars as measured by Filippenko et al. Object 6, with $V \approx 25.6$ mag, has colors consistent with a red supergiant, possibly as a result of substantial dust ($A_V \approx 4$ mag).

If SN 1961V were the giant eruption of an η Car analog, this still could not account for the non-thermal radio emission; η Car itself, for example, is a thermal bremsstrahlung radio source (e.g., Cox et al. 1995). From subsequent VLA observations in 1999 and 2000 Stockdale et al. (2001) confirmed the presence of nonthermal radio emission. Furthermore, Stockdale et al. claimed that the source had declined in flux since the previous radio observations (Branch & Cowan 1985). They inferred, once again, that SN 1961V is a fading, core-collapse radio SN. If the radio source were the SN, then Van Dyk et al. (2002) identified in shallow, archival *HST* Wide Field Planetary Camera 2 (WFPC2) images from 1994 and 2001 a fainter, red, possible optical counterpart in the environment, “Object 11.”

Chu et al. (2004) obtained *HST* Space Telescope Imaging Spectrograph (STIS) G430M and G750M grating spectra, along with an unfiltered 50CCD image, of the SN environment in 2002. They expected to detect emission lines, such as $[\text{O III}] \lambda 5007$, with high velocities, $> 2000\text{ km s}^{-1}$, from an old SN, e.g., as seen from SN 1957D (e.g., Long et al. 1992). Furthermore, if there were an old core-collapse SN in the field, detectable optical emission should accompany the nonthermal radio emission, as is the case generally for SNe (e.g., Chevalier & Fransson 1994). Chu et al. instead detected exactly *one* bright emission line, i.e., $\text{H}\alpha$, from exactly *one* point source within the $2''$ -wide slit. They measured a line width for the broad profile of $\lesssim 550\text{ km s}^{-1}$ full width zero intensity. To an astrometric accuracy of $\sim 0''.25$ using the STIS data, Chu et al. attributed the spectrum to Object 7, due to its coincidence with the SN optical position (Klemola 1986). They compared the $\text{H}\alpha$ line to that of η Car and concluded that this star is a possible LBV in the field. However, given the presence of the non-thermal radio emission, assumedly associated with an old SN 1961V, Chu et al. did not directly associate Object 7 with SN 1961V, except as a possible binary companion to the SN’s progenitor.

Van Dyk (2005) and Van Dyk & Matheson (2011) summarized and countered several of these arguments above, continuing to maintain the impostor status for SN 1961V. However, recently, two studies, Smith et al. (2011) and Kochanek et al. (2011), have concluded that SN 1961V was not an impostor, but, instead, a *bona fide* SN. Smith et al. base their conclusion on the relative energetics of the event and its apparent overall similarity to the SNe IIn, specifically the narrow emission-line widths and slow and unusual light curve. These authors argue that the high peak luminosity and high expansion velocity make it problematic for SN 1961V to conform to other presumed SN impostors and known LBVs. They argue that the light curve is consistent with the superpo-

sition of a normal Type II-Plateau SN light curve and a SN IIn-like light curve, with additional luminosity arising from enhanced interaction at late times with an existing circumstellar medium. Kochanek et al. rely almost entirely on an analysis of the mid-infrared dust emission in the SN environment. Their hypothesis is that, since the prediction is that a LBV survivor of SN 1961V would be cloaked by 4–5 magnitudes of visual extinction, this dust shell should be easily detectable in the thermal infrared (IR) as an IR η Car analog. The lack of detectable mid-IR emission at the SN position led Kochanek et al. to conclude that SN 1961V must have been a true SN, which has now faded below optical detectability.

3. OBSERVATIONS OF SN 1961V

There have been multiple observations of SN 1961V at a wide range of wavelengths in the last fifty years. Depending on the assumptions used in interpreting these data sets, one can come to several plausible conclusions. Here, and in § 4, we make the case that the overall picture across the electromagnetic spectrum is simpler and more consistent with SN 1961V as an eruptive LBV.

3.1. Radio Data

We obtained from the VLA data archive the 6 cm data, originally collected by Stockdale et al. (2001), and produced a map using standard routines in NRAO’s Astronomical Image Processing System (AIPS). We obtained from the *HST* archive the STIS 50CCD image from Chu et al. (2004) and applied a very accurate astrometric grid, $\pm 0''.02$ in both right ascension and declination, to the image, using the tasks *geomap* and *geotran* in IRAF¹. We then registered this image to our version of the radio map. This analysis first appeared in Van Dyk (2005).

The radio emission overlaid on the *HST* image is shown in Figure 1. The objects from Filippenko et al. (1995) and Van Dyk et al. (2002) are labeled in the figure. We place the accurate optical absolute position of SN 1961V (Klemola 1986) in the figure as well. It is clear from the figure that the optical SN position is most coincident with Object 7 (Chu et al. 2004 also pointed out this positional coincidence). However, the centroid of the radio source, which both Cowan et al. (1988) and Stockdale et al. (2001) claim to be associated with the SN, is significantly displaced, by $\sim 0''.4$ southeast (i.e., $\gtrsim 4\sigma$), from the optical position.

Furthermore, the nonthermal radio emission does not appear that well correlated with the stellar objects in the environment. Instead, we consider it far more likely that it is emission associated with what appears to be a complex, turbulent interstellar medium. Note the “finger” of radio emission that extends to the northeast from the main central concentration of emission, which appears to follow the arcs of nebular emission seen in the STIS image (Chu et al. 2004), which clearly includes nebular emission lines, alludes to such a spectacular interstellar environment (which is very conspicuous as being the

most optically luminous extranuclear emission region in the host galaxy). This is the “eastern H II region” from Fesen (1985; also Cowan et al. 1988) seen at much higher spatial resolution.

Additionally, our flux density measurement from the 2000 radio 6 cm data is 0.091 ± 0.005 mJy. Comparing this to 0.11 ± 0.03 mJy from 1986 (Cowan et al. 1988), it is not entirely obvious that the radio flux density had, in fact, actually declined in that time interval, as Stockdale et al. (2001) claimed. Therefore, we consider it to be quite convincing that the radio emission is not that of a fading radio SN, nor does the radio emission have any direct relation at all to SN 1961V.

3.2. *HST* Optical Data

We have analyzed archival *HST*/WFPC2 images, specifically of SN 1961V, obtained in 2008 August by program GO-10877 (PI: W. Li). These are exposures of 360 sec total in F555W and 800 sec total in F658N (the *HST* narrow band that includes H α at approximately the host galaxy redshift). The images are shown in Figure 2. The stars that are visible in the figure from Filippenko et al. (1995) and Van Dyk et al. (2002), again, are labeled. Admittedly not of the highest signal-to-noise ratio (S/N), it is clear from the figure that Object 7 is well detected in both bands (at 5.7σ in both F555W and F658N). In fact, Object 7 is the solitary H α source in the immediate central cluster. Object 10 (which from Figure 1 is most likely an emission region) and possibly another, unnumbered object to the northeast of Object 7, are the only other detected point-like sources in that image.

We measured photometry for these images using the routine HSTphot (Dolphin 2000a;b), which automatically accounts for WFPC2 point-spread function (PSF) variations and charge-transfer effects across the chips, zeropoints, aperture corrections, etc. HSTphot was run on both bands with a 3σ detection threshold. Object 7 is detected at $m_{F555W} = 24.70 \pm 0.19$ and $m_{F658N} = 20.45 \pm 0.19$ mag.

We can compare the m_{F555W} measurement for Object 7 from these 2008 data with that from the WF/PC-1 observations by Filippenko et al. (1995), i.e., $m_{F555W} = 24.22 \pm 0.07$ mag, and the WFPC2 F606W measurement by Van Dyk et al. (2002), i.e., $m_{F606W} = 23.84 \pm 0.14$ mag. Furthermore, we can measure the brightness of Object 7 from the archival STIS 50CCD image (normalizing to a 24-pixel-radius, or $1''.2$ -radius, aperture, which includes 100% of the encircled energy, following the online STIS Instrument Handbook), adopting the appropriate zero point for the clear (CL) bandpass from Rejkuba et al. (2000), and find $m_{CL} = 24.41 \pm 0.04$ (which is $\sim V$, if we assume $V - I \simeq 0.5$ mag). Although it is likely that we cannot directly compare observations made with *HST* with different detectors and different bandpasses to better than $\sim 10\%$, the m_{F555W} and m_{CL} all agree relatively well, while the m_{F606W} differs pretty significantly from the others. However, we have checked the photometry from Van Dyk et al. (2002) by running the images they analyzed through the most recent version of HSTphot and obtain $m_{F606W} = 24.44 \pm 0.19$ mag. This is quite different from the original, published value, but is far more in line with both of the m_{F555W} magnitudes. (We cannot readily explain why HSTphot now

¹ IRAF (Image Reduction and Analysis Facility) is distributed by the National Optical Astronomy Observatory, which is operated by the Association of Universities for Research in Astronomy, Inc., under cooperative agreement with the National Science Foundation.

produces a significantly different result than found by Van Dyk et al. 2002.) All-in-all, the $\sim V$ magnitudes for Object 7 are consistent, although we cannot completely rule out some variability or gradual fading of the source over nearly the last two decades.

We also obtained the STIS spectral data (Chu et al. 2004) from the *HST* archive and re-extracted the spectrum using standard STSDAS routines within IRAF. The portion of the spectrum including $H\alpha$ is shown in Figure 3. Although the spectrum is noisy, both a broad and a narrow component to the line are quite evident.

3.3. *Spitzer* Mid-Infrared Data

Similarly to Kochanek et al. (2011), we analyzed the archival mid-IR data for NGC 1058, obtained using the *Spitzer* Space Telescope with both the IR Array Camera (IRAC; 3.6, 4.5, 5.8, and 8.0 μm) and the Multi-band Band Photometer for *Spitzer* (MIPS; we analyzed the 24 μm data only). We considered the observations using both instruments from 2004 (GTO program 69; PI: G. Fazio) and from 2007 (GO program 40619; PI: R. Kotak), and assuming no variability for SN 1961V between these two epochs (if actually detected), we combined the data from these observations for each of the bands. The data we analyzed corresponded to pipeline versions S18.7 for IRAC and S18.12 for MIPS. We used the MOPEX (MOsaicking and Point source EXtraction; Makovoz & Khan 2005; Makovoz & Marleau 2005) package provided by the *Spitzer* Science Center to mosaic the individual Basic Calibrated Data (BCDs; in fact, for IRAC we used the artifact-corrected CBCDs) to produce a single image mosaic in each band (for both IRAC and MIPS, we left the first frame out of each set of observations when mosaicking, since it often has a far shorter exposure time than the rest of the BCDs and therefore adds mostly noise to the mosaic). We also applied the array location-dependent photometric corrections to the IRAC CBCDs within MOPEX, although, given the number of CBCDs and the adequate redundant coverage, this correction was not particularly important in the end. Although emission in all bands is detected from the environment of SN 1961V, the emission in the resulting mosaics is diffuse. As Kochanek et al. (2011) point out, neither Object 7 nor any of its immediate neighboring sources are detected in any of the *Spitzer* bands. Object 8, which is well separated from the SN 1961V position, dominates the emission from the environment at 8.0 μm . At 24 μm the spatial resolution is too poor to resolve which source, or sources, is the primary emitter in the environment. There is little point in analyzing the relatively low-resolution, low-sensitivity 70 μm data for the host galaxy.

We then used the routine APEX (Astronomical Point source EXtractor) Single Frame, with the “user list” input option, within MOPEX to perform aperture photometry at the exact position of SN 1961V. For the IRAC mosaics we used a 3.0-pixel-radius aperture, with an annulus for sky subtraction of radius 12.0–20.0 pixels, computing the sky background using the mode within the annulus. For the MIPS 24 μm mosaic we employed a 1.22-pixel-radius aperture, with sky annulus of radius 8.16–13.06 pixels. We applied the aperture corrections for the IRAC bands for our aperture/annulus configuration from the

online IRAC Instrument Handbook²). To determine the correction for the MIPS aperture, we had also performed point response function (PRF) fitting photometry on the mosaic. We considered the PRF fluxes of the two brightest stars, seen in the mosaic well away from the body of the galaxy, as “truth.” We then computed the ratio of the fluxes measured for these two stars through our aperture/annulus configuration and the PRF fluxes, i.e., 4.0:1.0, and corrected the aperture flux at the SN 1961V position by this ratio. All of these upper limits to the detection of SN 1961V are shown in Figure 4. (Since these are only upper limits, we dispensed with applying color corrections to both the IRAC and MIPS photometry.) Our limits are comparable to, although generally higher than, those that Kochanek et al. (2011) have estimated. The pertinent values with which to compare are those in their Tables 2 and 3, labelled “SN1961V area” (particularly, their 3''6-radius aperture measurements for IRAC), i.e., <0.026 , <0.022 , <0.079 , <0.230 , and <0.265 mJy (ours) *versus* <0.023 , <0.016 , <0.069 , <0.207 , and <0.226 mJy (theirs), at 3.6, 4.5, 5.8, 8.0, and 24 μm , respectively.

4. ANALYSIS

One of the assumptions made by Kochanek et al. (2011), as well as by Smith et al. (2011; and by earlier authors), is that the object detected in photographic plates back to the 1930s, prior to the 1960 “S Dor-type eruption” (Humphreys & Davidson 1994) and the 1961 luminous event was, in fact, the quiescent progenitor. We are now increasingly skeptical of this, and, instead, we find it far more compelling to presume that the precursor star was already in a state of sustained outburst prior to the more energetic eruption in the 1960s (see also Goodrich et al. 1989; Humphreys, Davidson, & Smith 1999). Clearly, this is difficult, if not impossible, to prove, due to the nonexistence of observations prior to the first available plates. However, the $B - V$ color ($\simeq 0.6$ mag) measured by Utrobin (1987) from the 1954 Palomar Sky Survey plates is essentially the same as the color during the outburst in 1961 and 1962 (Bertola 1965), and is the expected color of a LBV in an “eruptive state” (Humphreys & Davidson 1994). Furthermore, when the object was in its pre-outburst state at $m_{\text{pg}} \approx m_B \simeq 18$ mag, even assuming only Galactic foreground extinction ($A_V = 0.2$ mag; Schlegel et al. 1998), it had $M_{\text{bol}} \approx -12.6$ mag, which is well above the modified Eddington limit, $M_{\text{bol}} \simeq -11$ mag (e.g., Ulmer & Fitzpatrick 1998). The implication, therefore, is that the star was already super-Eddington in the decades leading up to the giant outburst. If Object 7 had an initial mass of $\sim 55\text{--}85 M_{\odot}$ (see below), then its present-day mass would be $\sim 25\text{--}40 M_{\odot}$ (from the models by Meynet & Maeder 2003) and, at its inferred present-day luminosity, $\sim 10^{5.8\text{--}6.2} L_{\odot}$ (see below), the star may be currently just at the Eddington limit for its mass.

We analyzed the STIS spectrum of Object 7, shown in Figure 3, by fitting the profile of the $H\alpha$ emission line with a pair of Lorentz profiles, one broad and one

² <http://ssc.spitzer.caltech.edu/irac/iracinstrumenthandbook/>, Table 4.7.

narrow, using the routine LMFIT within IDL³. The central wavelengths, λ_{cen} , for each of the profile components were allowed to roam during the fit. The resulting parameters are $\lambda_{\text{cen}} = 6580.78 \pm 0.80 \text{ \AA}$ and $\gamma = 6.83 \pm 1.45 \text{ \AA}$ for the broad component, and $\lambda_{\text{cen}} = 6579.19 \pm 0.04 \text{ \AA}$ and $\gamma = 0.40 \pm 0.04 \text{ \AA}$ for the narrow component. (The term γ is the FWHM scale parameter for the function.) The model fit is also shown in the figure. The velocity width of the broad component is then $\sim 311 \text{ km s}^{-1}$. The overall profile is asymmetric, as reflected in the slightly different λ_{cen} for the two components of the fit, with the profile appearing somewhat broader toward the red wing of the line than toward the blue wing.

The uncertainties in the 2008 F555W and F658N magnitudes for Object 7 are appreciable, and, unfortunately, no other recent broadband *HST* images exist to provide us with direct color information for the star (the SN 1961V environment is not detected in the F450W and F814W observations from 2007 by program GO-11119, PI: S. Van Dyk). Nonetheless, we attempt to produce a physically plausible and reasonably self-consistent model for Object 7 as an extinguished luminous blue emission-line star. We included the model emission line together with the model spectra of blue supergiants at LMC metallicity (Kochanek et al. 2011 consider the SN environment to be subsolar). The model supergiants were those from Kurucz (1993) within the STSDAS routine SYNPHOT in IRAF. Since the star has apparently declined in brightness only slightly over the years, we make the assumption that the star’s colors (in the WF/PC-1 bandpasses) have not varied from those measured in 1991, i.e., $m_{\text{F555W}} - m_{\text{F702W}} = 0.91 \pm 0.09$, $m_{\text{F555W}} - m_{\text{F785LP}} = 0.50 \pm 0.18$, and $m_{\text{F702W}} - m_{\text{F785LP}} = -0.41 \pm 0.18 \text{ mag}$ (see Filippenko et al. 1995, their Table 4). The coolest effective temperature (spectral type) the star could have, and still be responsible for photoionizing a putative surrounding nebula from which the $\text{H}\alpha$ emission arises, is $T_{\text{eff}} = 30000 \text{ K}$. We allowed the model to be as hot as $T_{\text{eff}} = 40000 \text{ K}$, approximately the highest effective temperature that supergiants in the LMC can attain (Massey et al. 2009).

We allowed the extinction to the model star also to vary, assumed a Cardelli, Clayton, & Mathis (1989) Galactic reddening law, corrected the model to the redshift of the host galaxy, and normalized the model to the m_{F555W} observed in 2008, all within SYNPHOT. In order for the resulting photometry from the model star to be constrained by the uncertainties in the WF/PC-1 colors, the assumed extinction could only vary from $A_V \simeq 1.8$ to 2.3 mag . One of the most important aspects of the model is that we can synthesize the observed F658N magnitude, without any further normalization, *exactly*. This is irrespective of the assumed temperature or extinction for the model, since the $\text{H}\alpha$ emission line dominates the model’s overall spectral energy distribution (SED).

The synthetic V magnitude of the model for Object 7, for the range of temperature and extinction, is 24.77 . For the range in extinction to the star and the distance to the host galaxy, this is a physically realistic $M_V^0 \simeq -6.9$ to -7.4 mag . (Note that this is quite comparable to the $M_V \simeq -7.4 \text{ mag}$ brightness for the precursor

of the modern impostor prototype, SN 1997bs in M66; Van Dyk et al. 2000). Integrating over the flux in the star models, after correcting for extinction and the distance to the host galaxy, we find that the bolometric luminosity is $L_{\text{bol}} \simeq 10^{(5.8-6.2)} L_{\odot}$. This range corresponds to bolometric magnitudes of $M_{\text{bol}} \simeq -9.8$ to -10.8 (assuming $M_{\text{bol}}(\odot) = 4.74 \text{ mag}$). The inferred range in bolometric corrections, $\text{BC}_V \simeq -2.9$ to -3.9 mag , is comparable to the BC_V found for O-type supergiants at LMC metallicity (Massey et al. 2009). We show the range in the hypothetical properties for the model star in Figure 5. In the figure we also show massive stellar evolutionary tracks from Lejeune & Schaerer (2001) for subsolar metallicity ($Z = 0.008$) at 120, 85, and $60 M_{\odot}$. It appears that the locus of Object 7 is of a star with initial mass $\sim 55\text{--}85 M_{\odot}$ near the point in the track where the star would evolve to the WR phase. Note that our model star is nowhere near as luminous, or as massive, as $\eta \text{ Car}$ (Humphreys & Davidson 1994; cf. their Figure 9).

The observed F658N brightness corresponds to an integrated flux in the model $\text{H}\alpha$ emission line, $F_{\text{H}\alpha} \simeq 6.3 \times 10^{-16} \text{ erg cm}^{-2} \text{ s}^{-1}$. Correcting for the host galaxy distance and the range of possible extinction, and also assuming $A_{\text{H}\alpha} = 0.81 A_V$ (e.g., Parker et al. 1992), the $\text{H}\alpha$ luminosity is in the range of $L_{\text{H}\alpha}^0 \simeq 2.5 - 3.6 \times 10^{37} \text{ erg s}^{-1}$. This is roughly comparable to the quiescent, although variable, luminosity $L_{\text{H}\alpha}^0 \approx 1.4 \times 10^{37} \text{ erg s}^{-1}$, for $\eta \text{ Car A}$ (Martin & Koppelman 2004; their Figure 5 — we have assumed the flux from that figure near maximum, i.e., $\sim 6 \times 10^{-9} \text{ erg cm}^{-2} \text{ s}^{-1}$), assuming the distance to $\eta \text{ Car}$ of 2.3 kpc and $A_V \sim 1.7 \text{ mag}$ to the central star (Davidson & Humphreys 1997).

The ionizing fluxes (in $\text{cm}^{-2} \text{ s}^{-1}$) from our model star would be $\log q_0 \simeq 23.5$ for $T_{\text{eff}} = 30000 \text{ K}$ and $\log q_0 \simeq 24.3$ for $T_{\text{eff}} = 40000 \text{ K}$ (Martins, Schaerer, & Hillier 2005). From the bolometric luminosity, above, the star would have a radius of $R \simeq 34 R_{\odot}$ for 30000 K and $\simeq 23 R_{\odot}$ for 40000 K . The number of Lyman continuum photons is then in the range of $\sim 2.2\text{--}6.6 \times 10^{49} \text{ s}^{-1}$. For Case B recombination, assuming an electron density $n_e \sim 10^2 \text{ cm}^{-3}$ and $\alpha_B \simeq 3 \times 10^{-13} \text{ cm}^3 \text{ s}^{-1}$, the Strömgren sphere for the star would be in the range $\simeq 3.9\text{--}5.6 \text{ pc}$. If the putative nebula around the star had been ejected at 2000 km s^{-1} (Zwicky 1964; Branch & Greenstein 1971; from a trace of the $\text{H}\alpha$ profile of the 1962 spectrum shown in Zwicky’s Figure 2, we confirm that the FWHM of the line is $\sim 4675 \text{ km s}^{-1}$, indicating that $v_{\text{exp}} \sim 1986 \text{ km s}^{-1}$) in an eruption that began at the end of 1960, then by 2008 August (the date of the most recent *HST* observations) the nebula would have expanded to $R_{\text{neb}} \simeq 3.0 \times 10^{17} \text{ cm}$, or $\simeq 0.1 \text{ pc}$. The nebula would therefore be easily photoionized. If we consider R_{neb} to be the Strömgren sphere radius, then the density of the nebula is probably more like $n_e \simeq 2.5\text{--}4.4 \times 10^4 \text{ cm}^{-3}$. We note that this is several orders-of-magnitude less dense than the $n_e > 10^7 \text{ cm}^{-3}$ limit placed on SN 1961V’s ejecta during outburst by Branch & Greenstein (1971; based on the lack of observed $[\text{Fe II}]$ lines), implying that the density has, naturally, declined as the ejecta have expanded over the decades. We also note that, assuming n_e , above, and a more likely value for R_{neb} (which we estimate below),

³ IDL is the Interactive Data Language, a product of Research Systems, Inc.

we find that $L_{\text{H}\alpha}^0 \simeq 6.7 \times 10^{37} \text{ erg s}^{-1}$, which is comparable to, yet about a factor of two larger than, what is observed; however, this also assumes a 100% recombination efficiency. The fact that the two estimates for the luminosity from the nebula are close lends credence to the combination of our estimates for the nebular radius and density.

We can use the relation between the ionized gas mass in the nebula and the (extinction-corrected) $\text{H}\alpha$ flux from Nota et al. (1992; who adapted this from Pottasch 1980, his Equation 5),

$$M_{\text{neb}}(M_{\odot}) = 3.87 \cdot (F_{\text{H}\alpha} [10^{-11} \text{ erg cm}^{-2} \text{ s}^{-1}]) \times (D [\text{kpc}^2])^2 (T_e [10^4 \text{ K}])^{0.85} (n_e [\text{cm}^{-3}])^{-1} \quad (1)$$

and assuming an electron temperature $T_e \simeq 10^4 \text{ K}$, and the ranges in both n_e and extinction, above, this results in $M_{\text{neb}} \approx 8\text{--}12 M_{\odot}$. If this nebula has been expanding at $v_{\text{exp}} = 2000 \text{ km s}^{-1}$, the resulting energy would be $E_{\text{kin}} = \frac{1}{2} M_{\text{neb}} v_{\text{exp}}^2 \approx 10^{50.6} \text{ erg}$. Assuming the conversion efficiency from kinetic to radiative energy is 10%, this can straightforwardly account for the total energy, $\approx 10^{49.6} \text{ erg}$, that Humphreys et al. (1999) estimated both $\eta \text{ Car}$ and SN 1961V had radiated during their mutual eruptions.

In their analysis, Kochanek et al. (2011) produced model SEDs for the mid-IR emission from a putative eruption survivor using DUSTY (Ivezic & Elitzur 1997; Ivezic, Nenkova, & Elitzur 1999; Elitzur & Ivezic 2001), assuming graphitic and silicate dust with properties from Draine & Lee (1984). Kochanek et al. assumed a spherical shell with an inner radius of $\simeq 1.3\text{--}1.5 \times 10^{17} \text{ cm}$ (which we show, below, is nearly a factor of two too small), and normalized the emission from the DUSTY models to a survivor brightness of $V = 24 \text{ mag}$ (which we have shown, above, is nearly a magnitude too bright). Their preferred scenario included an input source for the models having a temperature of 7500 K, which agrees with the colors for the object in 1954 measured by Utrobin (1987). The luminosity for the illuminating source at the shell's center, $L_{\star} \simeq 10^{6.9} L_{\odot}$, is, then, nearly an order-of-magnitude more luminous than what we have found for Object 7. These assumptions made by Kochanek et al. result in a dust shell with $A_V \sim 6\text{--}11 \text{ mag}$, which is considerably higher than even the estimates made by Goodrich et al. (1989) and Filippenko et al. (1995) of $\sim 4\text{--}5 \text{ mag}$, let alone the far more modest $A_V \simeq 1.8\text{--}2.3 \text{ mag}$ that we contend, above, is more likely for the survivor.

Kochanek et al. (2011) further argue that, even if one were to assume a model more similar to the quiescent LBV model which Goodrich et al. (1989) assumed (and to what we find likely to be the case for Object 7), i.e., $T_{\star} = 30000 \text{ K}$, $L_{\star} \approx 10^6 L_{\odot}$, and $A_V \simeq 2 \text{ mag}$ (corresponding to optical depths $\tau_V = 2.5$ and 4.5 for graphite and silicate dust, respectively, input into DUSTY), the resulting mid-IR emission would still be comparable to the emission from $\eta \text{ Car}$. That is, it would still be much higher in luminosity than the constraints imposed by the *Spitzer* data would allow (see their Figure 6). Again, these models were also normalized at nearly a magnitude brighter at V than what we have found for Object 7.

In spite of possibly inappropriate assumptions for the dust modeling, no reason exists in the first place to expect that SN impostors should generally be as dusty and as luminous in the mid-IR as $\eta \text{ Car}$. In Figure 4 we show the mid-IR fluxes we have measured from *Spitzer* archival data and presented in Van Dyk & Matheson (2011) for several SN impostors: SN 1954J/Variable 12 in NGC 2403, SN 1997bs, SN 1999bw in NGC 3198, and SN 2000ch in NGC 3432. We have adjusted the fluxes for all of these SN impostors to the distance of SN 1961V. For SN 1954J we have measurements from 2004 at 3.6 and 4.5 μm , but the flux in these bands may result from cool supergiants in that impostor's immediate environment (see Van Dyk et al. 2005); additionally, we obtain only upper limits to the emission at 5.8–24 μm . SN 1997bs is detected in 2004 only at 3.6 and 4.5 μm and is too confused in the longer-wavelength *Spitzer* bands. SN 1999bw was quite luminous in the mid-IR in 2004 (as shown in Figure 4), but subsequently faded in 2005 and 2006 (see also Sugerman et al. 2004). SN 2000ch may still have been in outburst when the *Spitzer* observations of its host galaxy were made in 2007 and 2008 (Pastorello et al. 2010), so a direct comparison with the quiescent SN 1961V is not warranted. Although none of these SN impostors was as luminous during eruption as SN 1961V (we note that the impostors are a diverse group of objects; e.g., Van Dyk & Matheson 2011; Smith et al. 2011), one can see that the SEDs, or limits to the SEDs, for all of these impostors are less luminous in the mid-IR than $\eta \text{ Car}$ (we show in Figure 4 the SED of $\eta \text{ Car}$, as detected by Morris et al. 1999 with the *Infrared Space Observatory*, scaled to the distance of SN 1961V). In particular, the detections and upper limits to the emission at the site of SN 1954J, which occurred nearly a decade before SN 1961V, are entirely consistent with the upper limits for SN 1961V. The oldest of the known SN impostors, $\eta \text{ Car}$, may simply be an “oddball,” in terms of the dust content of its Homunculus and its luminous mid-IR emission.

Furthermore, as we have already alluded to, we believe that the dust modeling by Kochanek et al. (2011) does not include the full range of complicating, but realistic, components. In particular, applying the interstellar graphite and silicate dust properties from Draine & Lee (1984) may not be appropriate for a LBV nebula. Evidence exists that the dust in these shells may be dominated by amorphous silicates, which we would expect for O-rich LBV nebulae enhanced in CNO-burning products (Umana et al. 2009; see also Lamers et al. 1996). We have therefore created two dust shell models, also using DUSTY, one with Fe-free Mg_2SiO_4 (forsterite) and the other with the olivine MgFeSiO_4 , which span essentially the range in expected optical depth for amorphous silicates in the wavelength range of interest. We have input to DUSTY the optical constants from Jäger et al. (2003) for the former and Jäger et al. (1994) and Dorschner et al. (1995) for the latter. If we assume material densities $\rho = 3.3 \text{ g cm}^{-3}$ for Mg_2SiO_4 and 3.7 g cm^{-3} for MgFeSiO_4 , we find opacities at V of $\kappa_V \simeq 7 \text{ cm}^2 \text{ g}^{-1}$ for Mg_2SiO_4 and $\simeq 3032 \text{ cm}^2 \text{ g}^{-1}$ for MgFeSiO_4 (with $\kappa_V = 3Q_{\text{abs}}/4\rho a$, where Q_{abs} is the dust absorption coefficient and a is the grain radius).

Additionally, if we infer from the SN 1961V light curve that the outburst ended sometime in 1962, then the ex-

pansion at 2000 km s^{-1} from this end date to the mid-date of the *Spitzer* observations, i.e., early 2006, leads to an inner radius for the dust sphere of $R_{\text{in}} \simeq 2.7 \times 10^{17} \text{ cm}$. If we also assume that the outburst commenced, roughly, at the end of 1960, then it effectively lasted for $\sim 2 \text{ yr}$, and the shell thickness $\Delta R \simeq 1.3 \times 10^{16} \text{ cm}$, or $\Delta R/R_{\text{in}} \simeq 0.05$. (As Weis 2003 has shown, the thickness of observed LBV nebulae, e.g. in the LMC, is generally $>10\%$; yet, as Kochanek et al. 2011 point out, the DUSTY models are relatively insensitive at these radii to the choice of shell thickness, and we find little difference in the results if we set $\Delta R/R_{\text{in}} > 0.05$.) If the mass of the gaseous nebular shell is $M_{\text{shell}} \simeq 10 M_{\odot}$ (see above), then, assuming a dust-to-gas ratio of 1/100, the shell's dust mass is $M_{\text{dust}} \simeq 0.1 M_{\odot}$, which, for optical depth $\tau_V = 3M_{\text{dust}}\kappa_V/4\pi R_{\text{shell}}^2$ and $R_{\text{shell}} = R_{\text{in}}$, results in $\tau_V \simeq 0.004$ and $\simeq 0.6$, respectively (which correspond in DUSTY to 0.133 and 1.083, respectively). Finally, we assume for the DUSTY modeling a Mathis, Rumpl, & Nordsieck (1977) dust grain size distribution (with index $q = 3.5$) and that the density distribution in the spherical shell around the central source varies $\propto r^{-2}$. If we represent Object 7 in DUSTY as a $T_{\text{eff}} = 30000 \text{ K}$ blackbody with luminosity $L \approx 10^6 L_{\odot}$, then the dust temperatures at the inner and outer edges of the shell are approximately 149 and 127 K, respectively, for the Mg_2SiO_4 model, and approximately 196 and 115 K, respectively, for the MgFeSiO_4 model.

Clearly, the values of τ_V for amorphous silicates in the shell are significantly smaller than those stemming from our assumed range in extinction, $A_V = 1.8\text{--}2.3 \text{ mag}$ (and are far smaller than what Kochanek et al. 2011 assumed for their primary scenario). As we have already emphasized, above, it is not necessary to presume that any nebula around SN 1961V is particularly dusty. For this reason, we further assume that the additional optical depth arises along the line-of-sight to SN 1961V within the host galaxy, and, therefore, we apply the “LMC average” extinction law from Weingartner & Draine (2001).

In Figure 4 we show our dust models, relative to the observed flux at V for Object 7 and the upper limits on the mid-IR emission from a dust shell. The prediction of the emission from the lower-optical-depth Mg_2SiO_4 dust model is comfortably within the observed upper limits, while, admittedly, the MgFeSiO_4 model predicts that SN 1961V should have been detected at $24 \mu\text{m}$, although it would escape detection in all of the IRAC bands (whereas all of the dust models by Kochanek et al. 2011 exceed the observed limits, at least at $8 \mu\text{m}$, if not in all of the IRAC bands). The situation for this latter model is further aggravated, of course, if we assume that Object 7 has $T_{\text{eff}} = 40000 \text{ K}$, increasing the overall mid-IR luminosity from the dust shell. Regardless of the star's effective temperature, one could sidestep the lack of detected $24 \mu\text{m}$ emission, however, by presuming, for instance, that the amorphous silicates in the shell are less Fe-rich, which is certainly possible. Another possibility is that the dust mass in the shell is less than what we have assumed, lowering the overall luminosity of the emission. Furthermore, the geometry of the ejected matter from Object 7 may be aspherical, asymmetric, or both (e.g., $\sim 50\%$ of known LBV nebulae appear to show a bipolar structure; Weis 2001). In any event, we have shown, using both ob-

servations of other SN impostors and what we consider to be a more realistic model of any dusty ejecta around the star, that the lack of mid-IR emission from SN 1961V alone, particularly across all of the *Spitzer* bands, is not a valid argument to eliminate the possibility altogether that it is a SN impostor.

5. CONCLUSIONS

Based on our analysis of the available data, we consider SN 1961V (still) to be a SN impostor and that Object 7 is the survivor of this event. All of the arguments we have made above, as part of this analysis, support this conclusion. We have also attempted to dispel several erroneous suppositions about the nature of this event. The survivor is clearly observed in very recent years to exist. The star quite plausibly has the properties of a quiescent, massive LBV. The star has not yet exploded and is not a radio SN. The star is surrounded by a circumstellar shell or nebula, however, this shell is not nearly as dusty as required by Kochanek et al. (2011) and previous investigators. We find that the visual extinction to Object 7 is in the range $A_V = 1.8\text{--}2.3 \text{ mag}$, and we suggest that most of this extinction is arising from the interstellar medium along our line-of-sight within the host galaxy, rather than from the shell itself. As a result, therefore, the shell need not be nearly as luminous an IR emitter as $\eta \text{ Car}$. This conclusion is further supported by the mid-IR observations of other SN impostors.

The positional proximity of Object 7 to SN 1961V, and the positional offset between SN 1961V and the radio source centroid, are both inescapable facts. The only conceivable way to counter the former fact is to conclude that Object 7 is either a physical or an optical double to the progenitor of an actual SN. This, of course, is possible. The uncertainty alone in the absolute position, $0''.1$, corresponds to $\sim 5 \text{ pc}$, certainly allowing for the possibility, in the relatively crowded cluster environment of SN 1961V, that Object 7 is merely a neighbor to the progenitor. Also, the probability of core-collapse SNe for high-mass stars in binaries is relatively high (e.g., Kochanek 2009). Although, if Object 7 were the binary companion to the star that exploded, we might expect Object 7 to have been stripped or otherwise affected by what would have been a very powerful explosion, potentially leading to an unusual brightness or color. This is not supported by the available photometry or inferred luminosity of Object 7. Instead, it appears to have the properties of a “run-of-the-mill,” evolved, high-mass star. Nonetheless, the positional offset between SN 1961V and the radio centroid is insurmountable — these two are not one and the same, which is essentially at the heart of the case that has been made for SN 1961V being a true SN.

No need exists for the supposed core-collapse explosion “hybrid” of a SN II-P and SN IIn. Furthermore, we disagree with the statement made by Smith et al. (2011) that SN 1961V is somehow unique among the impostors. It has direct analogs in both SN 2000ch (Wagner et al. 2004; Pastorello et al. 2010) and SN 2009ip in NGC 7259 (Smith et al. 2010; Foley et al. 2011), specifically in terms of the inferred expansion velocities at eruption and of the light curve behavior. The recent, more powerful revival of SN 2000ch displays “unusually” high velocities (FWHM) of $1500\text{--}2800 \text{ km s}^{-1}$ (Pastorello et al. 2010). SN 2009ip shows blueshifted He I absorption at

3000–5000 km s⁻¹, which Smith et al. (2010) speculate for SN 2009ip could be due to a fast blast wave, which occurred quasi-contemporaneously with the origin of the slower ejecta. SN 2000ch exhibits multiple P Cygni absorption components, with profile edges up to 3000–3500 km s⁻¹. A sustained high-luminosity pre-eruption state was seen for both SNe 2000ch and 2009ip; SN 2000ch was at $M_R \simeq -10.7$ mag prior to the 2000 eruption (Wagner et al. 2004), and SN 2009ip had a pre-eruption luminosity of $M_V \simeq -10$ mag (Smith et al. 2010). Although not nearly the $M_{\text{pg}} \approx -12$ mag brightness of SN 1961V, both SNe 2000ch and 2009ip, therefore, both may also have been in a super-Eddington phase prior to their giant eruptions. Even though the line widths were different, it is interesting to note that the H α line profiles, in particular, of SN 1961V (Zwicky 1964; see his Figure 2) and SN 2000ch (Wagner et al. 2004; see their Figure 7), near maximum of the 2000 eruption, were very similar — a sharp drop-off to the blue wing and extended wing to the red. The H α emission line in 2002 for Object 7/SN 1961V also showed a similar asymmetric profile (and, we emphasize that this profile had a very similar shape as the much broader line profile for SN 1961V in 1962, as shown by Zwicky). A possible explanation could be the effects of dust extinction in the expanding ejecta, although we have shown that the extinction from the ejecta is likely relatively modest for SN 1961V. A detailed analysis of this effect should be explored, although we consider this to be beyond the scope of this paper.

We do agree with Smith et al. (2011) and Kochanek et al. (2011), however, that the “undulations” in SN 1961V’s post-maximum light curve may well have arisen from the blast wave overtaking previously-ejected shells of matter ahead of the shock. We speculate here that the star was already in a sustained, eruptive outburst prior to 1960 and that the onset of the super-outburst, which peaked in luminosity in 1961 December, could possibly have been due to the interaction of the fast-moving (~ 2000 km s⁻¹), dense, massive shell with the pre-existing, slower, less dense mass loss. A potential analog is the behavior of the SN IIn 1994W in NGC 4041 — Dessart et al. (2009) modeled the high luminosity, sustained plateau, and sudden drop-off of this SN as the interaction of a fast ($\gtrsim 1500$ km s⁻¹), dense shell interacting with a slower, less dense shell. Furthermore, both the brief and more sustained plateaus in the SN 1961V light curve could have arisen from the interaction of the fast blast wave with various regimes of previously ejected matter, or to periods of partial recombination in the expanding ejecta, analogous to the recombination wave in SN II-P ejecta. Alternatively, these plateaus could also have been due to subsequent lesser eruptions by the star (Humphreys et al. 1999). The fast-moving massive shell radiated for many years after the super-outburst, albeit more faintly. Goodrich et al. (1989) detected the broad emission-line component at $F_{\text{H}\alpha} \simeq 2.2 \times 10^{-16}$ erg cm⁻² s⁻¹ in 1986.

We can set a limit on detection of this component in the *HST*/STIS spectrum from 2002 at $F_{\text{H}\alpha} < 3 \times 10^{-16}$ erg cm⁻² s⁻¹ (see Figure 3).

It is correct to point out the similarities in the variety of SN impostor and SN IIn properties. The two are very likely intimately intertwined, as we now know that at least one SN IIn arose from a SN impostor (SN 2005gl; Gal-Yam et al. 2007, Gal-Yam & Leonard 2009). The SN IIn are also a diverse class of objects (if the term “class” is truly applicable in the case of such heterogeneity), and it is still not clear how many SNe IIn have, in fact, really been impostors. For instance, SN 1994W itself may be an impostor (Dessart et al. 2009).

Obviously, we have extrapolated fairly extravagantly from two photometric measurements of Object 7 from recent *HST* data. We have had to assume that the colors for the star from 1991 are applicable to 2008 as well. What is ultimately required is a set of deep, multiband optical and near-IR observations of the SN 1961V environment using the modern *HST* with the Wide Field Camera 3, which would vastly improve upon the pre-furbishment WF/PC-1 images and the motley assortment of WFPC2 and unfiltered STIS image data analyzed to date. Such future observations would only require a rather modest investment of *HST* time — to image in *BVRIZH* at $S/N \gtrsim 10$ would require only 3 orbits. Looking beyond *HST*, observations with the *James Webb Space Telescope*, particularly with the Mid-IR Instrument (MIRI), would reveal the actual dust emission from the surviving star. This object has clearly garnered much attention and speculation over the decades and continues to provide us with invaluable insights into the evolution of the most massive stars. With these space-based data, the definitive nature of the SN 1961V precursor may well be established once and for all.

Finally, NGC 1058 should continue to be regularly monitored by SN searches in nearby galaxies. For Object 7 as the SN 1961V survivor, we might expect, much as was the case for SN 2006jc (Foley et al. 2007; Pastorello et al. 2007), that the star will *truly* explode as the SN that we believe other authors have erroneously concluded has already occurred. The super-outburst from the 1960s could well be the forerunner of a core-collapse event. It is possible that the star will explode as a high-luminosity, hydrogen-rich SN IIn, such as SN 2006gy (Ofek et al. 2007; Smith et al. 2007), or as a more helium-rich SN Ibn, such as SN 2006jc (as suggested by Kochanek et al. 2011).

This work is based in part on archival data obtained with the *Spitzer Space Telescope*, which is operated by the Jet Propulsion Laboratory, California Institute of Technology under a contract with NASA. We thank Roberta Humphreys, for her comments, and the referee, whose recommendations helped improve the manuscript. We also thank Chris Kochanek for correcting us on our use of “ τ ” in the DUSTY modeling.

Facilities: VLA, HST, Spitzer.

REFERENCES

- Bertola, F. 1964, *Ann. Ap.*, 27, 319
 Bertola, F. 1965, *Contr Asiago Obs* 171
 Branch, D., & Greenstein, J. L. 1971, *ApJ*, 167, 89
 Branch, D., & Cowan, J. J. 1985, *ApJ*, 297, L33
 Cardelli, J. A., Clayton, G. C., & Mathis, J. S. 1989, *ApJ*, 345, 245

- Chevalier, R. A. & Fransson, C. 1994, *ApJ*, 420, 268
- Chevalier, R. A. 2003, in *From Twilight to Highlight: The Physics of Supernovae*, eds. W. Hillebrandt & B. Leibundgut (Berlin: Springer),
- Chu, Y.-H., Gruendl, R. A., Stockdale, C. J., et al. 2004, *AJ*, 127, 2850
- Cowan, J. J., Henry, R. B. C., & Branch, D. 1988, *ApJ*, 329, 116
- Cox, P., Mezger, P. G., Sievers, A., et al. 1995, *A&A*, 297, 168
- Crowther, P. A. 2007, *ARA&A*, 45, 177
- Davidson, K. & Humphreys, R. M. 1997, *ARA&A*, 35, 1
- Dessart, L., Hillier, D. J., Gezari, S., Basa, S., & Matheson, T. 2009, *MNRAS*, 394, 21
- Dolphin, A. E. 2000a, *PASP*, 112, 1383
- Dolphin, A. E. 2000b, *PASP*, 112, 1397
- Dorschner, J., Begemann, B., Henning, T., Jäger, C., & Mutschke, H. 1995, *A&A*, 300, 503
- Draine, B. T., & Lee, H. M. 1984, *ApJ*, 285, 89
- Elitzur, M., & Ivezić, Z. 2001, *MNRAS*, 327, 403
- Fesen, R. A. 1985, *ApJ*, 297, L29
- Filippenko, A. V. 1997, *ARA&A*, 35, 309
- Filippenko, A. V., Barth, A. J., Bower, G. C., et al. 1995, *AJ*, 110, 2261 [Erratum: 1996, *AJ*, 112, 806]
- Foley, R. J., Smith, N., Ganeshalingam, M., et al. 2007, *ApJ*, 657, L105
- Foley, R. J., Berger, E., Fox, O., et al. 2011, *ApJ*, 732, 32
- Gal-Yam, A., Leonard, D. C., Fox, D. B., et al. 2007, *ApJ*, 656, 372
- Gal-Yam, A., & Leonard, D. C. 2009, *Nature*, 458, 865
- Goodrich, R. W., Stringfellow, G. S., Penrod, G. D., & Filippenko, A. V. 1989, *ApJ*, 342, 908
- Humphreys, R. M., & Davidson, K. 1994, *PASP*, 106, 1025
- Humphreys, R. M., Davidson, K., & Smith, N. 1999, *PASP*, 111, 1124
- Ivezic, Z., & Elitzur, M. 1997, *MNRAS*, 287, 799
- Ivezic, Z., Nenkova, M., & Elitzur, M. 1999, *User Manual for DUST*, University of Kentucky Internal Report, accessible at <http://www.pa.uky.edu/~moshe/dusty>
- Jäger, C., Mutschke, H., Begemann, B., Dorschner, J., & Henning, T. 1994, *A&A*, 292, 641
- Jäger, C., Dorschner, J., Mutschke, H., Posch, T., & Henning, T. 2003, *A&A*, 408, 193
- Kiewe, M., Gal-Yam, A., Arcavi, I., et al. 2012, *ApJ*, 744, 10
- Klemola, A. R. 1986, *PASP*, 98, 464
- Kochanek, C. S. 2009, *ApJ*, 707, 1578
- Kochanek, C. S., Szczygiel, D. M., & Stanek, K. Z. 2011, *ApJ*, 737, 76
- Kurucz, R. 1993, *ATLAS9 Stellar Atmosphere Programs and 2 km/s grid*. Kurucz CD-ROM No. 13. Cambridge, Mass.: Smithsonian Astrophysical Observatory, 1993
- Lamers, H. J. G. L. M., Morris, P. W., Voors, R. H. M., et al. 1996, *A&A*, 315, L225
- Lejeune, T., & Schaerer, D. 2001, *A&A*, 366, 538
- Long, K. S., Winkler, P. F., & Blair, W. P. 1992, *ApJ*, 395, 632
- Makovoz, D., & Khan, I. 2005, *Astronomical Data Analysis Software and Systems XIV*, 347, 81
- Makovoz, D., & Marleau, F. R. 2005, *PASP*, 117, 1113
- Martin, J. C., & Koppelman, M. D. 2004, *AJ*, 127, 2352
- Martins, F., Schaerer, D., & Hillier, D. J. 2005, *A&A*, 436, 1049
- Massey, P., Zangari, A. M., Morrell, N. I., et al. 2009, *ApJ*, 692, 618
- Mathis, J. S., Rumpl, W., & Nordsieck, K. H. 1977, *ApJ*, 217, 425
- Meynet, G., & Maeder, A. 2003, *A&A*, 404, 975
- Morris, P. W., Waters, L. B. F. M., Barlow, M. J., et al. 1999, *Nature*, 402, 502
- Nota, A., Leitherer, C., Clampin, M., Greenfield, P., & Golimowski, D. A. 1992, *ApJ*, 398, 621
- Ofek, E. O., Cameron, P. B., Kasliwal, M. M., et al. 2007, *ApJ*, 659, L13
- Parker, J. W., Garmany, C. D., Massey, P., & Walborn, N. R. 1992, *AJ*, 103, 1205
- Pastorello, A., Smartt, S. J., Mattila, S., et al. 2007, *Nature*, 447, 829
- Pastorello, A., Botticella, M. T., Trundle, C., et al. 2010, *MNRAS*, 408, 181
- Pottasch, S. R. 1980, *A&A*, 89, 336
- Rejkuba, M., Minniti, D., Gregg, M. D., et al. 2000, *AJ*, 120, 801
- Schlegel, E. M. 1990, *MNRAS*, 244, 269
- Schlegel, D. J., Finkbeiner, D. P., & Davis, M. 1998, *ApJ*, 500, 525
- Silbermann, N. A., Harding, P., Madore, B. F., et al. 1996, *ApJ*, 470, 1
- Smith, N., & Owocki, S. P. 2006, *ApJ*, 645, L45
- Smith, N., Li, W., Foley, R. J., et al. 2007, *ApJ*, 666, 1116
- Smith, N., Chornock, R., Li, W., et al. 2008, *ApJ*, 686, 467
- Smith, N., Miller, A., Li, W., et al. 2010, *AJ*, 139, 1451
- Smith, N., Li, W., Silverman, J. M., Ganeshalingam, M., & Filippenko, A. V. 2011, *MNRAS*, 415, 773
- Stockdale, C. J., Rupen, M. P., Cowan, J. J., Chu, Y.-H., & Jones, S. S. 2001, *AJ*, 122, 283
- Sugerman, B., Meixner, M., Fabbri, J., & Barlow, M. 2004, *IAU Circ.*, 8442, 2
- Turatto, M., Cappellaro, E., Danziger, I. J., et al. 1993, *MNRAS*, 262, 128
- Ulmer, A., & Fitzpatrick, E. L. 1998, *ApJ*, 504, 200
- Umana, G., Buemi, C. S., Trigilio, C., et al. 2009, *ApJ*, 694, 697
- Utrobin, V. P. 1984, *Ap. Space Sci.*, 98, 115
- Utrobin, V. P. 1987, *Soviet Astronomy Letters*, 13, 50
- Van Dyk, S. D. 2005, in *The Fate of the Most Massive Stars*, eds. R. Humphreys & K. Stanek (ASP, San Francisco), 47
- Van Dyk, S. D., Filippenko, A. V., Chornock, R., Li, W., & Challis, P. M. 2005, *PASP*, 117, 553
- Van Dyk, S. D., & Matheson, T. 2011, in *Eta Carinae and the Supernova Impostors*, eds. R. M. Humphreys & K. Davidson (Springer, Heidelberg), in press
- Van Dyk, S. D., Weiler, K. W., Sramek, R. A., et al. 1996, *AJ*, 111, 1271
- Van Dyk, S. D., Peng, C. Y., King, J. Y., et al. 2000, *PASP*, 112, 1532
- Van Dyk, S. D., Filippenko, A. V., & Li, W. 2002, *PASP*, 114, 700
- Wagner, R. M., Vrba, F. J., Henden, A. A., et al. 2004, *PASP*, 116, 326
- Weingartner, J. C., & Draine, B. T. 2001, *ApJ*, 548, 296
- Weis, K. 2001, *Reviews in Modern Astronomy*, 14, 261
- Weis, K. 2003, *A&A*, 408, 205
- Zwicky, F. 1964, *ApJ*, 139, 514

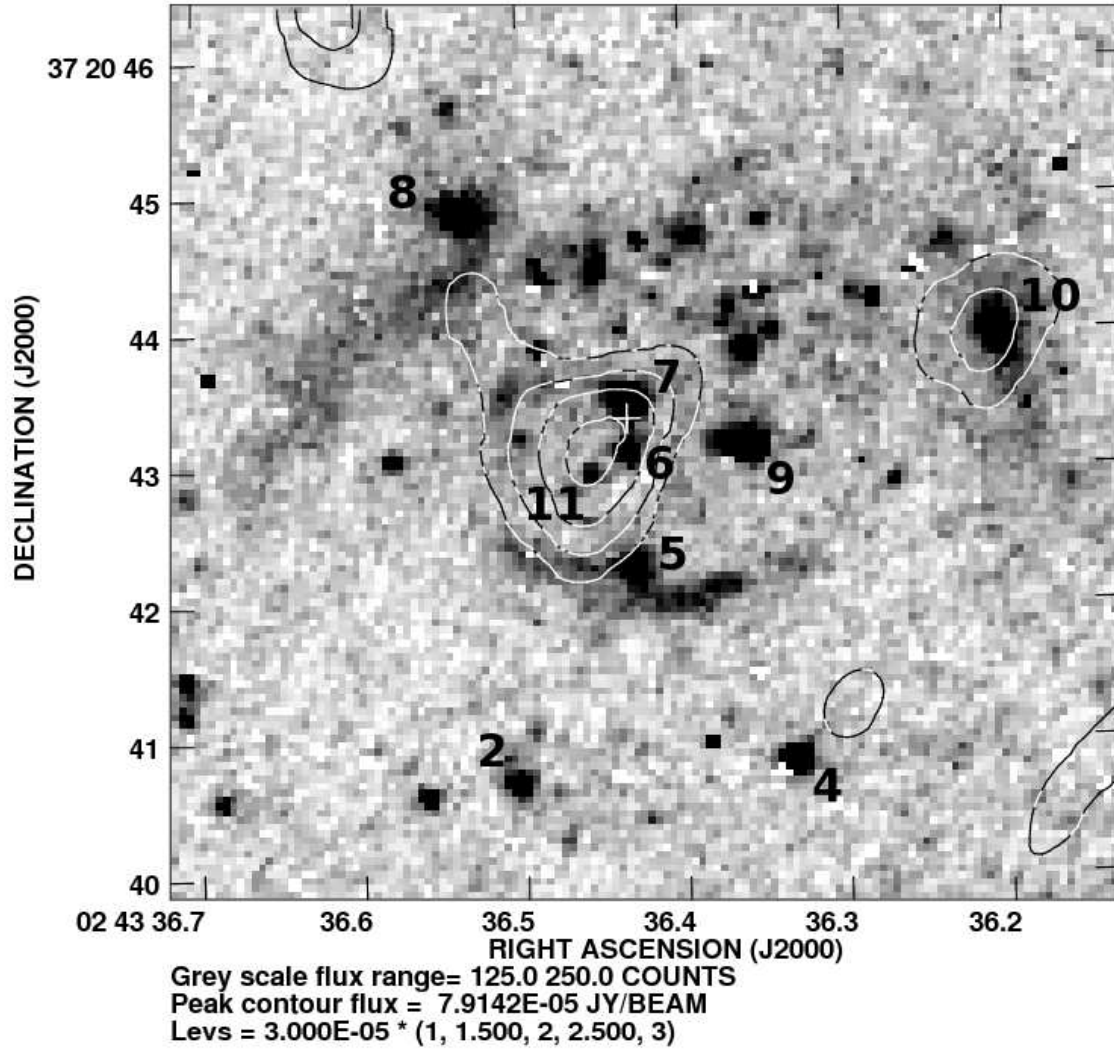


FIG. 1.— *HST*/STIS unfiltered 50CCD image of the SN 1961V site from Chu et al. (2004), obtained from the archive. Source numbering is the convention from Filippenko et al. (1995) and Van Dyk et al. (2002). The *contours* are the 6 cm radio data from Stockdale et al. (2001), which we have reanalyzed. Contour levels are (1, 1.5, 2, 2.5, 3) $\times 0.03$ mJy/beam. The *white cross* represents the accurate absolute optical position of SN 1961V from Klemola (1986) and is shown at $2\times$ the actual positional uncertainty.

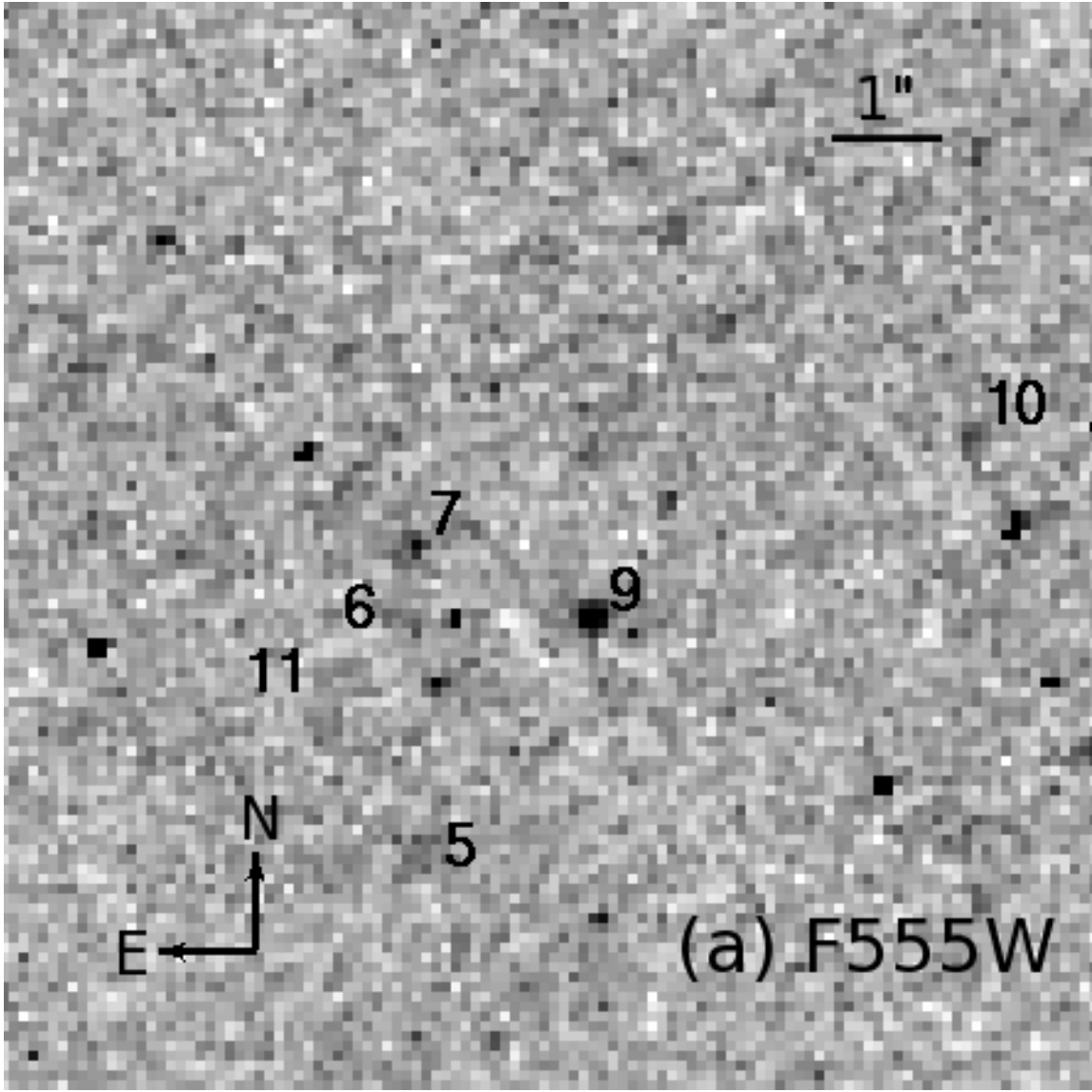


FIG. 2.— *HST*/WFPC2 image of the SN 1961V site from 2008, obtained from the archive, (a) in F555W, and (b) in F658N. Source numbering is the convention from Filippenko et al. (1995) and Van Dyk et al. (2002). North is up, and east is to the left.

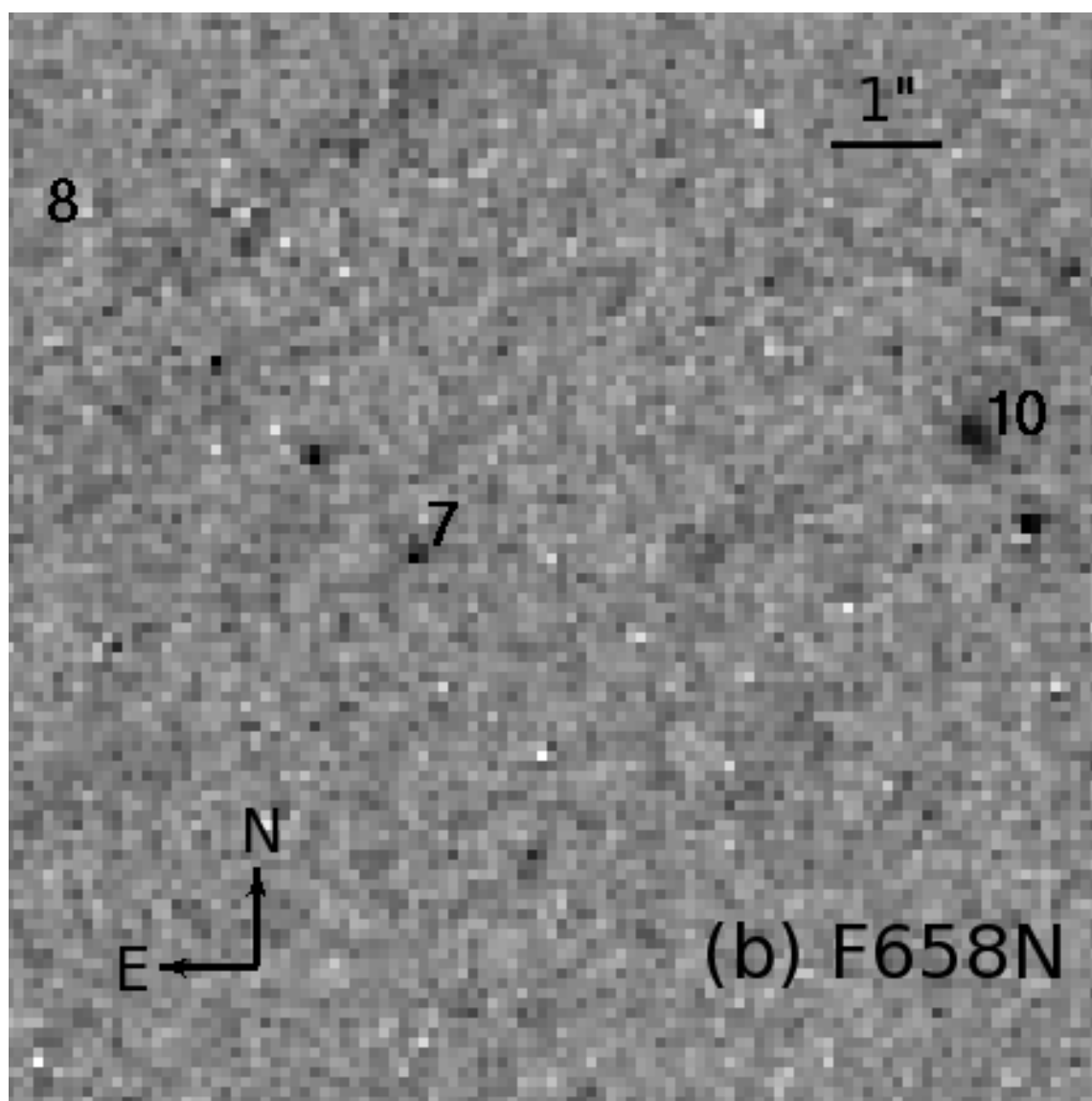


FIG. 2.— Continued.

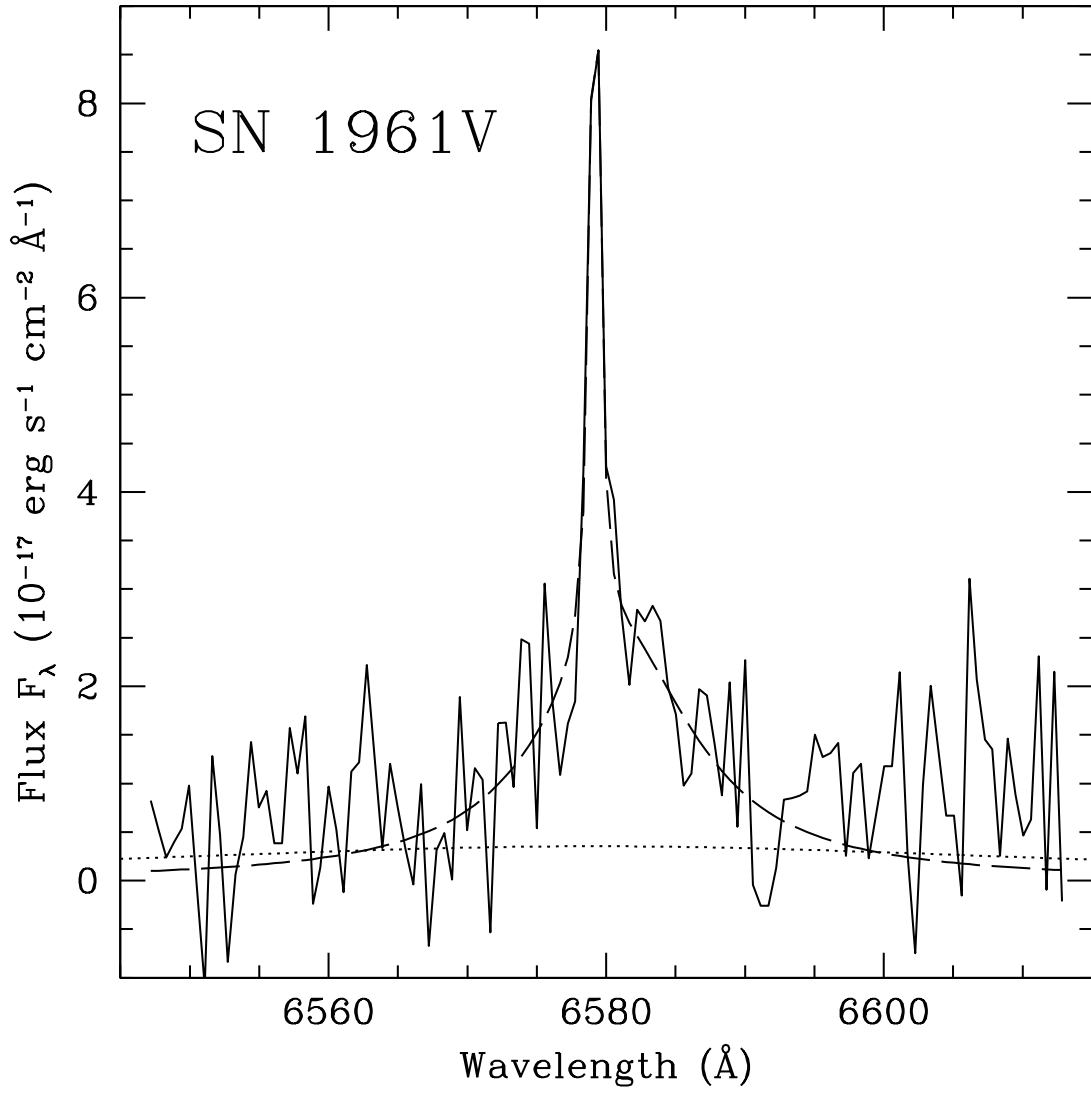


FIG. 3.— A re-extraction of the *HST*/STIS spectrum (*solid line*) of SN 1961V obtained by Chu et al. (2004) in 2002, showing the only distinct emission line visible in that spectrum, i.e., H α . We have fit both the broad and narrow profiles of the line with the combination of two Lorentz functions (*dashed line*; see text for details). We also show the limit on the detection of the very broad (~ 2000 km s $^{-1}$) component to the emission line (*dotted line*), first observed by Zwicky (1964) and later by Goodrich et al. (1989).

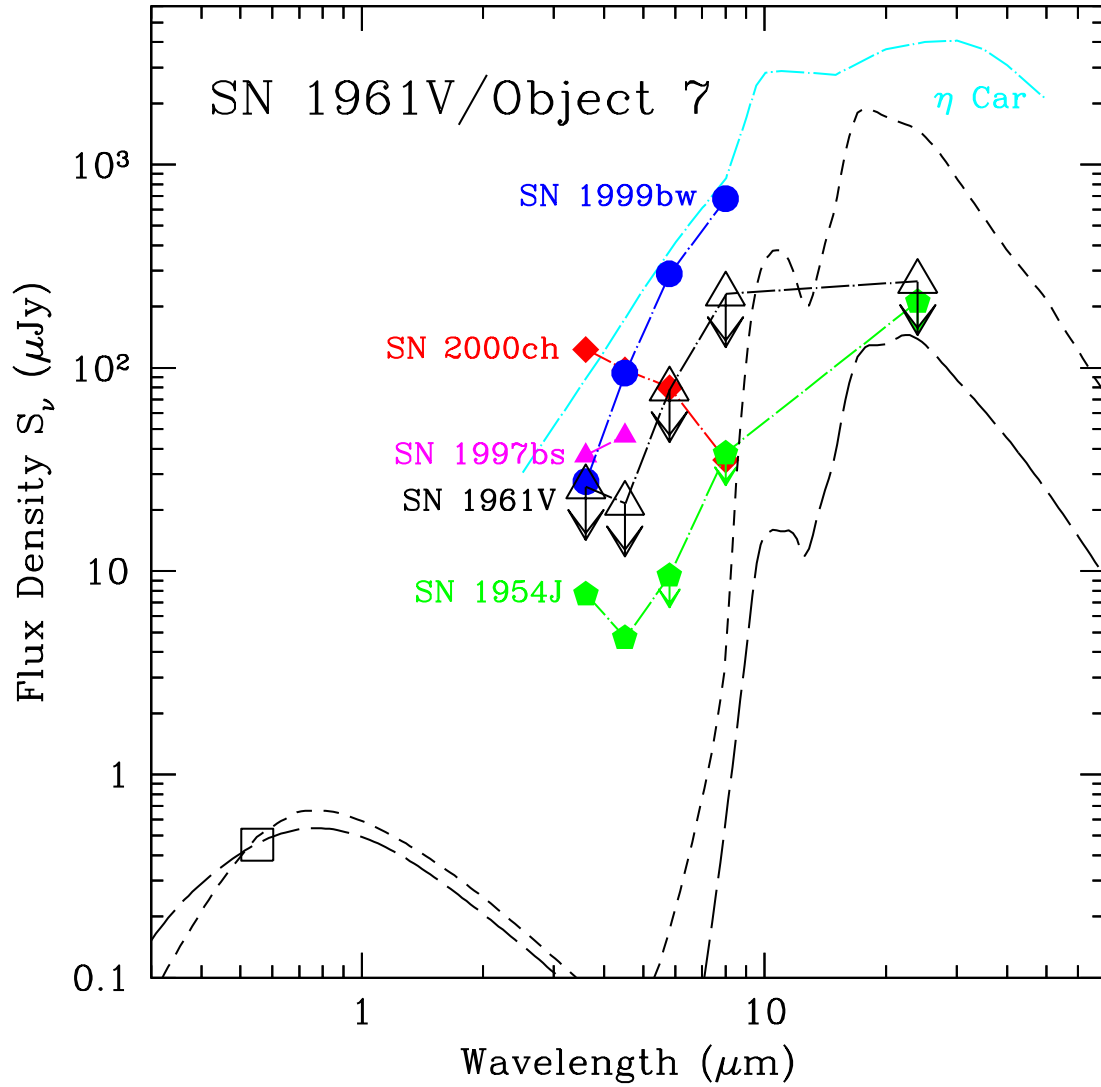


FIG. 4.— Upper limits to the flux densities in the *Spitzer* IRAC and MIPS 24 μm bands (*open triangles*) at the exact position of SN 1961V (Klemola 1986). Also shown are measurements (and upper limits to detection) in some or all of these bands (Van Dyk & Matheson 2011) for the “impostors” SN 1954J/Variable 12 (*green filled pentagons*), SN 1997bs (*magenta filled triangles*), SN 1999bw (*blue filled circles*), and SN 2000ch (*red filled diamonds*). Additionally, we show the observed SED for η Car (Morris et al. 1999; *cyan dot-dashed line*). Finally, we show model SEDs generated using DUSTY (Ivezic & Elitzur 1997; Ivezic, Nenkova, & Elitzur 1999; Elitzur & Ivezic 2001), assuming a spherical shell of inner radius $R_{\text{in}} \approx 2.7 \times 10^{17}$ cm and thickness $\Delta R/R_{\text{in}} = 0.05$, around a central illuminating source assumed to be a $T = 30000$ K blackbody with luminosity $L \approx 10^6 L_\odot$; the dust in the shell is assumed to consist of amorphous silicates, either Mg_2SiO_4 (Jäger et al. 2003; *long-dashed line*) or MgFeSiO_4 (Jäger et al. 1994, Dorschner et al. 1995; *short-dashed line*). We also assume additional extinction, following the “LMC average” law from Weingartner & Draine (2001), in the foreground within the host galaxy along our line-of-sight. The total visual extinction for the models is assumed to be the midpoint value in the range $A_V = 1.8\text{--}2.3$ mag, and the models are normalized to the $V = 24.77$ mag brightness of the SN 1961V survivor, Object 7 (*open square*). See text.

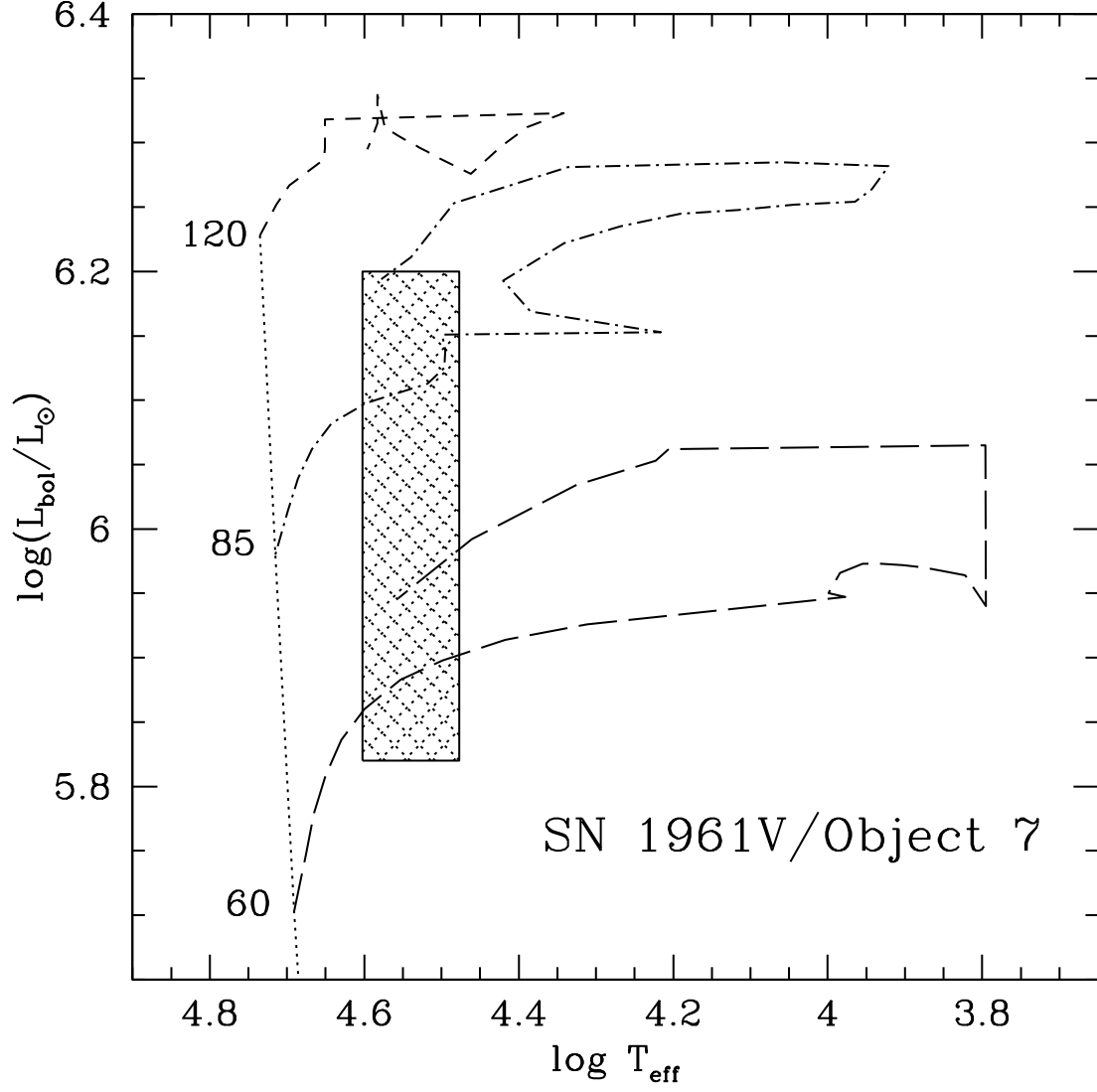


FIG. 5.— Hertzsprung-Russell diagram, showing the approximate locus of properties for our hypothetical model survivor of SN 1961V at quiescence (*shaded region*). Also shown are theoretical evolutionary tracks for subsolar metallicity ($Z = 0.008$) at 120 (*short-dashed line*), 85 (*dot-dashed line*), and 60 M_{\odot} (*long-dashed line*), from Lejeune & Schaerer (2001). This figure intentionally emulates a similar figure in Humphreys & Davidson (1994; their Figure 9) for direct comparison.